



IGY BULLETIN

SEP 18 1960
CHICAGO

A monthly survey of programs and findings of the International Geophysical Year and the International Geophysical Cooperation—1959 as related primarily to United States programs. The Bulletin also reports on international programs in geophysics and space science that have grown out of the IGY, and on their results.

Severe Sea Surges at Barbados

The following material is based on a more detailed report by William L. Donn and William T. McGuinness, both of the Lamont Geological Observatory of Columbia University, which was published in the December 1959 issue of the Journal of Geophysical Research.

To obtain a better understanding of both long- and short-term variations in sea level, networks of island observatories were set up in the Atlantic and Pacific Oceans as part of the IGY Oceanography Program. Tide gauges and wave meters at these observatories kept a continuous record of sea-level fluctuations; standard meteorological measurements were also obtained to provide data on possible relationships between atmospheric and oceanic phenomena. (*Bulletin No. 22* reports on some preliminary results of the Atlantic Ocean investigations, which were conducted under the direction of the Lamont Geological Observatory, and refers to earlier reports outlining the island observatory program and describing some of the instrumentation used.)

The island of Barbados, in North Atlantic equatorial waters near the lower end of the British West Indies, was the site of an island observatory during the IGY (see Fig. 1). The coasts of Barbados, as well as of other West Indian islands, have frequently suffered successions of unusually high and often damaging sea waves. These sea surges were not associated with local or Caribbean storms, and attempts to explain them as

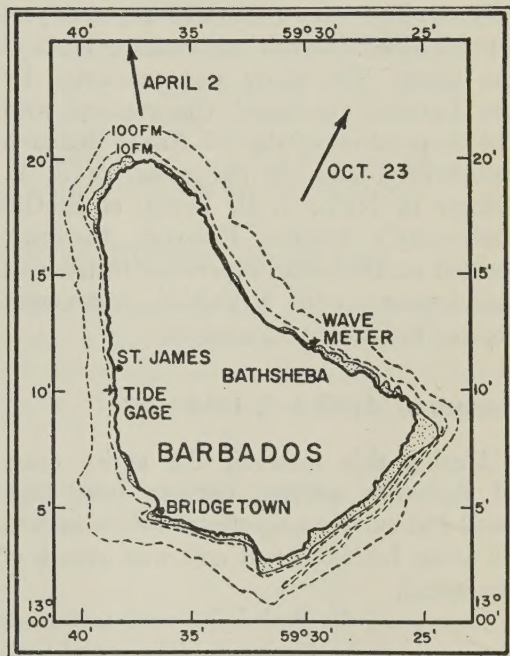


Fig. 1. Island of Barbados, British West Indies. Instrument locations and directions toward swell-generating regions of North Atlantic storms (arrows) are shown.

tsunamis—great sea waves produced by submarine earthquakes or volcanic activity—or as the result of submarine landslides, have been unsuccessful.

The lack of precise observational data on the physical characteristics of such waves has in the past been a major deterrent to a satisfactory explanation of their origin. On the basis of data obtained at the

Barbados IGY island observatory, however, it is now apparent that these severe coastal disturbances result directly from high sea swells radiating from remote storms over the North Atlantic at middle latitudes. This report describes and analyzes several occasions during the IGY when such high and damaging surf conditions occurred along the coasts of Barbados.

Observations used in the investigation were obtained by a wave meter installed in about 80 feet of water off Bathsheba, on the east coast of Barbados, and by a standard tide gauge at St. James, on the west coast (Fig. 1). The wave meter was emplaced just outside the coral reef surrounding most of the island. The study was conducted by the Lamont Geological Observatory with the cooperation of the US Naval Research Laboratory, and, in particular, of J. E. Dinger of NRL. J. B. Lewis, of McGill University's Bellaire Research Institute, located on Barbados, supervised instrument maintenance and forwarded instrument records to Lamont for analysis.

Surges of April 4-6, 1958

During this interval, the entire coast of Barbados suffered damage from high swell and surf; strong effects were observed all along both the east and west coasts of the island.

Data from the Bathsheba wave meter are summarized in Figure 2. The amplitude curve, which represents the significant wave height (the average of the highest one-third of the waves), shows the first increase above background just prior to 2400 GMT on April 3. Maximum wave height occurred at about 1800 on April 5, almost two days after the onset. Wave period, which increased at about the time of the first height increase, reached a maximum of 15 seconds shortly before the time of maximum wave height. (The plotted period represents the average of the periods of the dominant waves measured over a 10-minute interval every two hours.)

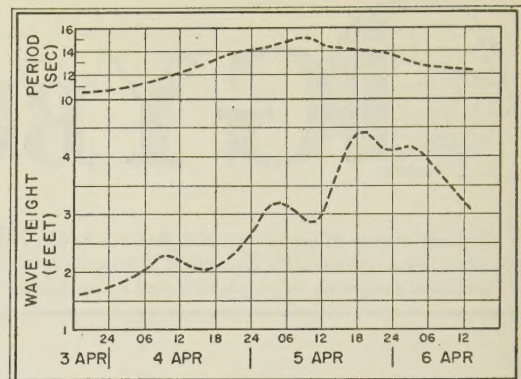


Fig. 2. Record of Wave Height and Wave Period from the Bathsheba Wave Meter, April 3-6, 1958.

The St. James records for this interval reinforce those obtained at Bathsheba. Comparison of the records from both locations shows that the interval of high waves occurred at nearly the same time on both sides of the island.

It thus appears that the damaging surf originated from typical but strong ocean swell, and this, in turn, suggests a probable storm origin. Although no directional data are available for the swell, the absence of any tropical or subtropical storms in nearby oceanic areas indicates a more remote origin. According to North Atlantic weather charts, a large, intense, extratropical cyclone traveled northeastward after originating off Cape Hatteras on March 31. On April 1 and 2, 45- to 50-knot winds prevailed over a fairly long southerly fetch (distance over the water) in the western half of the storm. Figure 3 shows the storm's position on the morning of April 2.

The relation of the Barbados swell to this storm is shown by using travel times for the waves corresponding to two points on the wave curves (Fig. 2), one near the beginning of the heightened wave activity and one at maximum. The wave period at 0800, April 4, was 11.5 seconds. Using a group velocity of 16.75 knots, position arcs (isochrones) were constructed along a line extending from Barbados in the direction from which the swells were coming (see

Fig. 4). The arcs mark prior intervals of 12 hours.

When compared with the positions of possible generating areas shown on the weather charts, the isochrone for 1800, March 31 (A, Fig. 4), appears to correspond well with the position of the storm at that time. Similarly, if a group velocity of 22.5 knots is used for the 15-second waves at 0900 on April 5, it is evident that the isochrone of the wave position for 0600, April 2 (B, Fig. 4), intersects the intense storm area at about the same time. A discrepancy of 2 to 3 hours in precise meeting of the waves and storm is well within the experimental error of the procedures involved, particularly as the weather charts are issued at only 6-hour intervals.

As the storm moved northeastward, the position of best fit kept pace. It thus seems definite that the Barbados swell of April 4-6, 1958, originated in this coastal storm and that the longer-period and higher waves were generated later in the storm, when the storm had moved northeastward and was at a somewhat greater distance from the station.

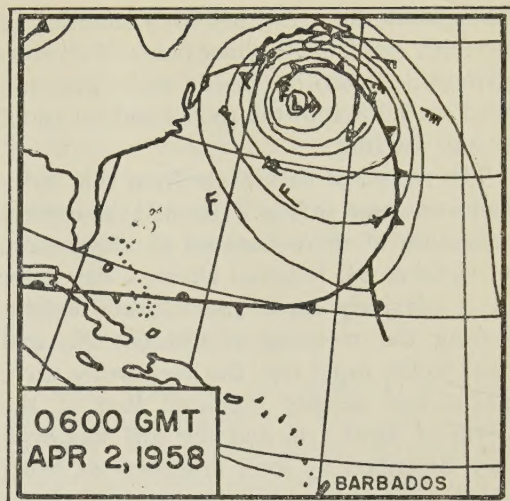


Fig. 3. Weather Chart of North Atlantic Storm on April 2, 1958. Isobars indicate six-millibar pressure intervals; arrows fly with the wind, each full barb representing a speed of 10 knots and each flag 50 knots.

Surges of October 24-28, 1958

On October 25 and 26, 1958, the east coast of Barbados was again battered by extremely high, unusually severe surf. Waves up to 30 feet in height pounded the coast

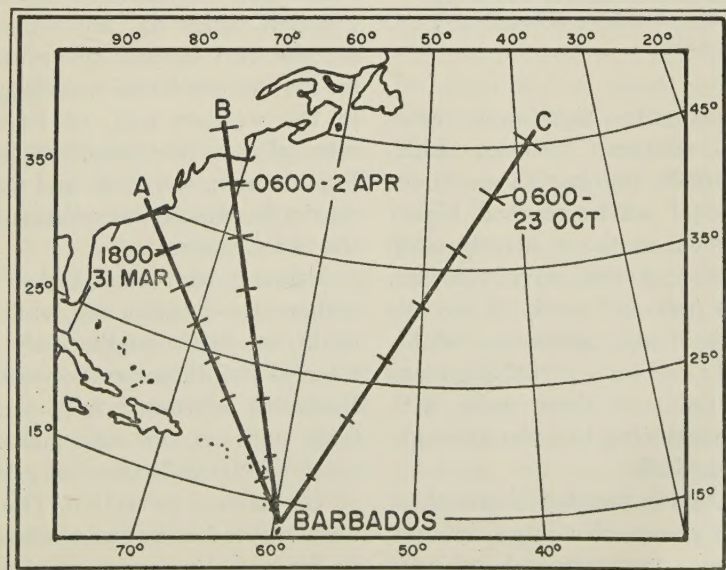


Fig. 4. Position Arcs (Isochrones) for Barbados Storm Swell in Early April (paths A and B) and Late October (path C), 1958.

throughout the night and early morning of the 25th and 26th. Fishing boats of all sizes were hurled onto the beach, and water and sand cascaded into the rooms and cellars of coastal dwellings.

The record of this storm from the Bathsheba wave meter (Fig. 5) showed the earliest indication of wave increase at about 1200 on October 24, followed about a day later by a relatively rapid rise in wave height. During the morning of October 25, and prior to the rapid rise, the deep-water wave height had already exceeded that of the storm of April 4-6, and the surf was even then described by local fishermen as being of record height.

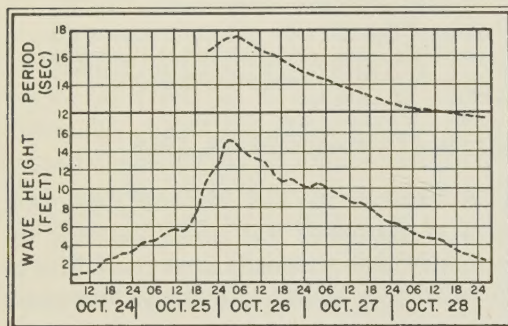


Fig. 5. Record of Wave Height and Wave Period from the Bathsheba Wave Meter, October 24-28, 1958.

Although maximum significant wave height, which occurred between 2400, October 25, and 0600, October 26, was about 15 feet, individual waves reached higher than 18 feet even in the relatively deep water at the site of the wave recorder. Maximum wave period of nearly 18 seconds was simultaneous with maximum height. Both wave height and wave period decreased slowly during the next three days, with record heights continuing to occur throughout October 26 and 27.

The North Atlantic weather charts show the growth and decay of a large, intense, low-pressure area (extratropical cyclone) between October 22 and 25. During the two days of maximum intensity (October 23

and 24) the storm moved very slowly, with the center remaining close to 40° N, 40° W.

Using a group velocity of 27 knots for the waves of maximum period at the time of Barbados wave maximum, it was found that good coincidence of swell and storm occurred during the morning of October 23 (C, Fig. 4). The swell isochrone for 0600 intersects the storm area at just that time, indicating that the maximum Barbados swell probably originated in this storm at a time when the storm was large and intense. As the storm was nearly stationary, the resulting waves were more strongly affected by the fetch, duration, and speed of the wind than if the storm had moved at the more usual 20- to 30-knot speed toward the northeast.

No reports of unusual surf were made for the west coast of Barbados during this interval of record seas along the eastern shores, as was the case on April 4-6.

Comparison of April and October 1958 Storm Effects

The swell at Barbados from the storms of April and October 1958 differed in both magnitude and distribution. Although the reported winds did not differ significantly for the two storms, the pressure gradient for the October storm was distinctly stronger in the western half, at least during the interval centered around 1800, October 23. Furthermore, the fetch and the duration of maximum winds, were distinctly greater for the October storm.

Although somewhat higher wind speeds, and greater duration and fetch of the winds, could at least qualitatively account for some of the difference between the swell at Barbados associated with these storms, a large part remains unexplained. However, much of the difference may be explainable on the basis of refraction. The directions of wave travel for the two storms are indicated in Figure 1 by arrows pointing toward the storms. Clearly, the swell from the April storm, arriving from the north, would

spread southward along both the east and west coasts of Barbados but would suffer considerable refraction in the process of developing surf along the shore. It is quite evident from air photographs of refracted swell that the resulting extension of the wave crests may result in considerable decrease in amplitude. Some change in period is also likely.

Swell from the October storm, arriving from the northeast, would strike much more directly on the east coast, with relatively little refraction, while the west coast would be mostly sheltered from this swell. Although severe extratropical cyclones with appropriate fetch to produce high Barbados rollers, as in early April 1958, may occur in North Atlantic coastal areas a few times a year, mid-ocean storms like that of October 1958 are much more rare, as are cases of extremely high Barbados swell such as that generated by this storm.

Qualitatively, at least, the difference between the distribution and magnitude of the swell of the April storm and of the October storm thus seems explainable on the basis of refraction and sheltering. Adequate shore data are not available at present for evaluating these effects quantitatively.

Tidal Effects

The relationship between the occurrence of storm swell and the phase and range of tide seems also to be of importance in determining shore effects. The difference between the range of the spring and neap tides at Barbados (St. James) is about two feet. (Spring-tide range is three feet and neap-tide range is one foot). The high surf of April 4-6 occurred at exactly the time of spring tide and that of October 25-26 occurred about halfway between spring and neap tides.

Normal swell, particularly at times of low tide or neap tide, tends to break on the reef and leave the shore unmolested. Swell arriving at spring tide can clear the reef

and break on shore during high water. High swell arriving during the high phase of spring tide thus becomes a threat. Even the effects of the very high swell of October 25-26 were modulated by the tide phase, with the severest effects reported on the afternoon of the 25th and early morning of the 26th, at the times of high tide.

Other Recent Surges Observed at Barbados

Other cases of high surf at Barbados occurred during May 3-5, 1958, and December 7-9, 1957. Owing either to incomplete installation or to temporary breakdown of wave-recording equipment, complete wave records of these storms were not obtained. However, on the basis of available data, the appropriate North Atlantic weather charts were examined and it was found that two intense storms existed in the western North Atlantic at these times. Winds exceeding 50 knots and similar in location and behavior to those of the storm of April 1958 were reported.

Conclusions

Storm rollers and high surf at Barbados and in the Lesser Antilles in general, that are not related to local storms, appear to be generated in large and intense extratropical cyclones at middle latitudes in the North Atlantic Ocean. By simply monitoring weather charts of the North Atlantic Ocean it should be possible to make qualitative forecasts of the arrival of the storm swell in the Barbados area at least two or three days in advance. The swell may be expected to be especially high if it arrives during spring tides.

Further detailed study, including wave-spectrum determination and refraction corrections, will be necessary in order to make possible the quantitative forecasting of the precise arrival time, height, and period of the storm swell.

From the studies conducted thus far, it appears that storms to the north (off the

eastern coast of the United States) generate swell that affects both sides of Barbados but suffers considerable amplitude loss from refraction. It is probable, on the other hand, that swell from mid-ocean storms of great intensity principally strike the eastern coast with an effect that is a function of size, intensity, and route of travel of the storm.

The explanation of the Barbados sea surges as originating in distant storms places them in a class with the well-known rollers of the South Atlantic and Indian oceans. These long-period rollers, also of distant-storm origin, can produce breakers and surf reaching 40 feet in height on the coasts of islands in these oceans.

Radioactive Tracer Studies of Mixing in the Atlantic Ocean

The following material is based on a report by V. T. Bowen, of Woods Hole Oceanographic Institution, and T. T. Sugihara, of Clark University. The original, more-detailed, account appeared in Nature, April 2, 1960.

The circulation and mixing of ocean waters are extremely important to man, exerting a very powerful influence on climate and largely controlling the fertility of marine life. Man's knowledge of this circulation and mixing is still quite limited, but in recent years a new tool—radioactive "tracers"—has been found which promises to add greatly to this knowledge. These tracers, consisting of minute particles of natural and artificial radioactive nuclear materials, can be followed for great distances in the atmosphere and oceans, providing much new data on the space and time patterns of their motions.

The IGY program included radioactive-tracer studies of both the air and the oceans. *Bulletins 14 and 16* present background information on these studies, and some preliminary findings. The present report is concerned with some results in the marine program. The work described was part of a Woods Hole Oceanographic Institution

IGY project supported by the National Science Foundation, the Office of Naval Research, and the Atomic Energy Commission.

In previous investigations of the geochemistry of carbon dioxide in the oceans, and of ocean mixing as determined by carbon-14 distribution, the ocean waters have customarily been separated into shallow surface reservoirs and deep reservoirs. The shallow surface reservoirs are assumed to be well mixed, while the deep reservoirs are assumed to be only slowly renewed from the surface.

In some applications, the quantitative expression of this two-reservoir concept is extremely sensitive to the depth of the surface reservoir and to its rate of mixing with the waters below it. These factors can be determined by use of relatively short-lived radio-isotopes added to the surface layer from above. In both the North and South Atlantic, strontium-90 (half-life 28 years, as compared to 5568 years for carbon-14) permits such determinations as it has been added to the sea water in measurable quantities only at the surface. Moreover, this strontium-90 is completely soluble in sea water and the concentration is not changed significantly by either biological or chemical processes. Its vertical

Table 1. Strontium-90 in the North and South Atlantic

Depth (meters)	Location and Date						
	15° 49' S, 35° 50' W (4/1-2/57)	8° 26' S, 7° 45' W (3/1/57)	16° 15' N, 43° 37.5' W (11/22/57)	36° 23' N, 70° 33' W (7/13/57)	31° 15' N, 68° 10' W (12/8/57)	34° 30' N, 65° 42' W (7/11-12/58)	34° 39' N, 67° 24' W (7/15-16/58)
0	4.1 ± 0.5	5.0 ± 1.0	6.3 ± 0.6	10.5 ± 0.6	10.9 ± 0.6	7.6 ± 0.6	9.1 ± 0.6
100			5.4 ± 0.5		7.7 ± 0.6	13.0 ± 0.7	8.2 ± 0.6
300		2.4 ± 1.0				11.8 ± 0.9	5.5 ± 0.5
400			2.2 ± 0.3		3.9 ± 0.6		
500				4.1 ± 0.6		7.3 ± 0.4	6.4 ± 0.5
700		<0.3			2.3 ± 0.4	3.7 ± 0.5	3.4 ± 0.5
1000	1.5 ± 0.6			<1.0		<0.9	1.7 ± 0.3
1200			1.6 ± 0.8				

Note: Concentrations of Sr⁹⁰ are given in disintegrations per minute per 100 liters of ocean water.
 Deviations indicated are those expected from counting statistics only.

transport depends, therefore, entirely on the vertical component of motion of the water in which it is dissolved.

As part of a continuing program of analysis of marine radio-isotopes, a number of series of measurements have been obtained of the change with depth of the strontium-90 concentration. Table 1 includes the results of seven series of strontium-90 analyses, showing very significant radiostrontrium concentrations at depth in the Atlantic Ocean, both north and south of the equator. Although there are still too few analyses for very precise determinations, an average concentration of about half the surface value is indicated for depths between 300 and 700 meters. The upper 100 meters, as generally assumed, appears well mixed, and the concentration falls off sharply between 100 and 300-to-400 meters. Appreciable concentrations are common at depths between 1000 and 1200 meters, but the investigators found no measurable radiostrontrium in samples from depths of 3000 to 5000 meters.

In the water columns sampled thus far, there appears to be three to four times as much total strontium-90 below a depth of 100 meters as above. It is reasonable to assume, moreover, that all of this strontium-90 has been added since mid-1954. Thus, the possibility that this vertical transport may have taken place by sinking along density surfaces appears to be completely eliminated by the short time available and the great horizontal distances that would have had to be traversed. Instead, a more-or-less direct vertical movement resulting from wind-driven mixing is indicated.

As shown in Table 1, there was close agreement between the strontium-90 concentrations of the 400- and 500-meter samples obtained in the Sargasso Sea region on July 13 and December 8, 1957, while significantly higher values were found in this region in July of 1958. This suggests that vertical transport takes place mostly during the winter, when surface water cools and wind velocities are high.

Measurements of Carbon Dioxide in the Atmosphere

The following material is based on a report by Charles D. Keeling, of the Scripps Institution of Oceanography, University of California. The more detailed account appeared in Tellus, June 1960.

A coordinated effort was made during the IGY and IGC-1959, by scientists of the Scripps Institution of Oceanography, the Woods Hole Oceanographic Institution, Lamont Geological Observatory, the University of Washington, and Texas Agricultural and Mechanical College, to determine the amount, distribution, and variations of carbon dioxide in the earth's atmosphere. (*Bulletins 16* and *20* present background information on the program and some early results.)

Although the CO₂ content of the atmosphere is comparatively small, it has an important influence on world climate. Ultra-violet and infra-red radiations from the sun are mostly absorbed in the earth's atmosphere—ultraviolet by oxygen at high levels, and infrared by CO₂ and water vapor at low levels. Most visible radiations, however, penetrate to the surface of the earth, where they are mainly reflected back to the atmosphere if they fall on snow or ice, or mainly absorbed if they fall on land or water. The visible radiations falling on land or water are heated in the process of absorption and are then re-radiated as infrared radiation, which is, in turn, partially absorbed in the lower atmosphere by CO₂ and water vapor, thus warming the air. This is the so-called "greenhouse effect," and one aim of the IGY program has been to attempt to ascertain whether man, in burning increasing quantities of fossil fuels (coal, oil, etc.), is causing this greenhouse effect to become intensified, with resulting long-range climatic changes.

It was found prior to the IGY that the

content of CO₂ in the atmosphere, in contrast to oxygen, nitrogen, and the rare gases, is significantly variable. Later data has indicated that the variability is smaller and more systematic than previously believed.

This report presents preliminary results of investigations of atmospheric CO₂, carried out as part of the IGY and IGC-59 program. These studies show a systematic variation in the concentration of CO₂ with season and latitude in the Northern Hemisphere, but a small, steady increase in concentration in Antarctica.

Figure 6 shows the locations of CO₂ recording stations and the tracks of oceanographic research cruises and aircraft flights on which measurements were made during

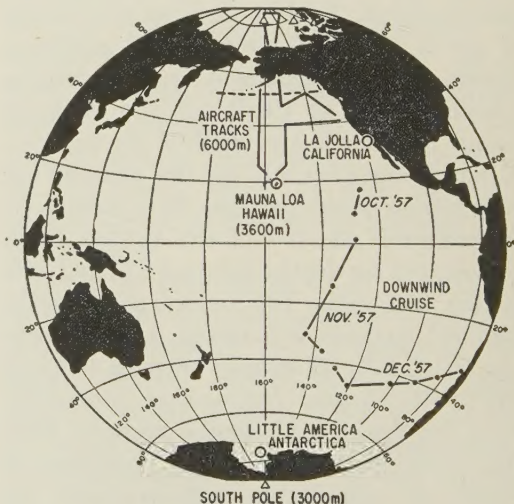


Fig. 6. IGY-IGC Stations and Ship and Aircraft Tracks for Sampling of Atmospheric CO₂. Circles denote continuous-recording stations; triangles are those on Arctic Ocean drifting stations and at IGY South Pole Station. Elevations are given in meters for locations more than 100 meters above sea level; dotted line indicates approximate mean position of limiting temperature isotherm used to separate aircraft data into groups associated with higher and lower air temperature.

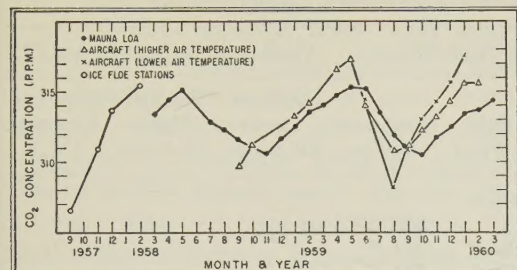


Fig. 7. Variation in Concentration of Atmospheric CO_2 in the Northern Hemisphere, 1957-1960.

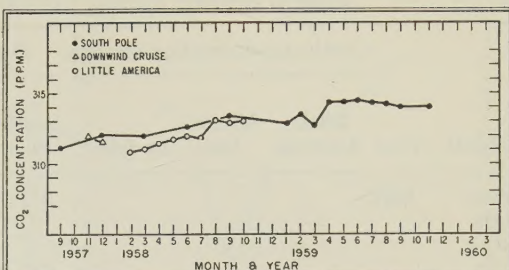


Fig. 8. Variation in Concentration of Atmospheric CO_2 in the Southern Hemisphere, 1957-1960.

the IGY-IGC under the direction of the Scripps Institution of Oceanography. US Weather Bureau personnel carried out sampling at the IGY Little America and Amundsen-Scott South Pole stations in Antarctica, at Mauna Loa Observatory in Hawaii, and at IGY Drifting Stations Alpha and Bravo, in the Arctic Ocean. C. E. Williams and J. C. Pales, of the Weather Bureau, operated the continuous-recording instruments at Little America and Mauna Loa, respectively, and reduced data to preliminary tabular form. The 55th Weather Reconnaissance Squadron of the US Air Force collected samples from aircraft; Maj. G. T. McClelland, Maj. B. M. Rose, Lt. R. E. Nagle, Lt. H. T. Fukuda, and Capt. J. D. Sharp were especially instrumental in planning and executing this work. N. W. Rakestraw and Lee Waterman collected samples during the Downwind Expedition, conducted by Scripps in the Southeast Pacific in the fall and winter of 1957-58 (see *Bulletins 7 and 16*).

Procedure

Three gas analyzers equipped with strip-chart recorders were employed during the IGY and IGC-59 to measure continuously the concentration of CO_2 at the stations in Antarctica, Hawaii, and California. A fourth analyzer was used in the laboratory to analyze samples of air collected in glass flasks at various locations. These analysers provide direct comparisons between the

partial pressure of CO_2 in air (that part of total atmospheric pressure exerted by carbon dioxide) and that in prepared mixtures of CO_2 in nitrogen gas.

The relative accuracy of the data presented here is approximately ± 0.3 parts per million by volume. The uncertainty in the absolute values is considerably larger, however, since only a preliminary calibration of the reference mixtures has been made. When an accurate calibration is completed, the absolute accuracy is expected to approach ± 0.1 ppm. Monthly averages of the data from the continuously recording stations and from collections in flasks are presented numerically in Table 1 and plotted in Figures 7 and 8.

Results

Local contamination was found in the vicinity of all three continuous-recording stations. At Little America Station, it was evidently caused solely by combustion of fuel in the immediate vicinity of the station. It could be readily spotted from the significant fluctuations in the otherwise steady trace of the recorder pen and was eliminated from consideration in the initial reading of the charts.

At Mauna Loa Observatory, a less prominent variability was found in approximately half the records. This is attributed to release of CO_2 by nearby volcanic vents; to combustion associated with agricultural, industrial, and domestic activities on the

Table 2. Monthly Average Concentrations of Atmospheric Carbon Dioxide*

Month	Year	Continuous Recording Stations			Surface Flask Samples			Flask Samples from Aircraft***		
		Little America	Mauna Loa	La Jolla**	South Pole	Arctic Ice Floes	Downwind Cruise	Data at Lower Air temp.	Data at Higher Air temp.	Limiting Air temp. (°C.)
Sept	1957				311.1	306.5				
Oct							310.9**			
Nov						310.8	311.9			
Dec					312.0	313.6	311.6			
Jan	1958									
Feb		310.8								
Mar		311.0	313.4			311.9	315.5			
Apr		311.4	314.4	314.3				314.9**		-27
May		311.7	315.1	315.3						
Jun		311.9				312.5		314.9**		-21
Jul		311.8	312.9	311.1						
Aug		313.0	312.3	308.4						
Sept		312.9	311.6	308.7	313.3			308.3**	309.6	-18
Oct		313.0		310.8				312.8**	311.2	-27
Nov			310.6	313.2						
Dec			311.6	314.3						
Jan	1959		312.5	314.9	312.8			313.2		-36
Feb			313.5	314.4	313.4			314.1		-36
Mar			314.0	315.4	312.7					
Apr			314.7	315.0	314.3			316.6**	316.6	-27
May			315.3	315.0	314.3				317.3	-24
Jun			315.2	315.2	314.4			314.3	314.1	-21
Jul			313.5	311.5	314.2					
Aug			311.9	308.1	314.2			308.1	310.7	-18
Sept			311.1	308.7	314.0			311.0	311.1	-27
Oct			310.5	312.1				313.0	312.1	-27
Nov			311.8	313.7	313.9			314.2	313.2	-36
Dec			312.5	313.5				315.6	314.3	-36
Jan	1960		313.4	314.7				317.6	315.6	-36
Feb			313.7	315.4					315.6	-36
Mar			314.4	314.7						

* In ppm of dry air by volume

** Data not shown in Figures 2 or 3

*** Data separated into two groups based on temperature of the air at point of sampling. Limiting air temperature refers to the temperature separating the lower air-temperature group from the higher. It was chosen so that, for each sampling period, the boundary between warmer and colder air lies at approximately 50° N (see Fig. 7).

island; and to a lower concentration of CO₂ in air transported to the station by upslope winds. The values reported here are averages of data for periods of down-

slope winds or strong lateral winds, when the concentration remained nearly constant for several hours or more.

At La Jolla, California, the concentration

was found to be highly variable. Highest concentrations occurred when light winds blew from the north (from the direction of Los Angeles); concentrations were lowest when the wind was from the west or southwest and of moderate force or greater. Lowest weekly values usually did not differ by more than ± 1 ppm during any month and, within a range of 2 ppm, agreed with values obtained by aircraft in the northern Pacific Ocean. Monthly averages of these data, which presumably indicate nearly uncontaminated air, are cited in Table 1.

Data for air collected in flasks from aircraft flying at 5 to 6 kilometers above the Pacific and Arctic Oceans and from surface stations at the South Pole and on Arctic ice floes show a high degree of regularity.

A clearly defined seasonal trend in concentration is found at all locations in the Northern Hemisphere. The annual range of concentration becomes greater from south to north and the month of minimum concentration occurs earlier. When the aircraft samples are separated into two groups based on air temperature at the point of sampling (Table 2), values for the high-latitude, or polar, air are seen to have a greater seasonal range than comparable values for air of the temperate zone. In contrast, data for the Southern Hemisphere do not indicate any seasonal variation. Data obtained on the Downwind Cruise in November and December 1957 suggest that the concentrations observed over Antarctica prevail at all southern latitudes of the Pacific Ocean.

The seasonal trend in concentration observed in the Northern Hemisphere (Fig. 9) may result from the activity of land plants. In the temperate zone, maximum concentrations have been found to occur in spring, at the outset of the growing season for plants, and minimum concentrations occur in the fall, approximately at the end of the growing season. The absence of a seasonal trend in the Southern Hemisphere may then be a result of the smaller area covered by growing plants at temperate and polar

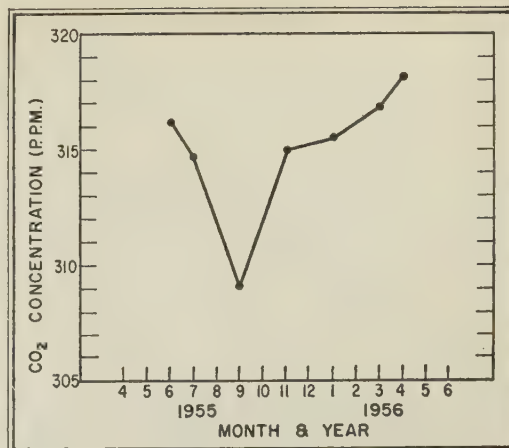


Fig. 9. Variations in Concentration of Atmospheric CO₂. (Based on data by C. D. Keeling for various locations near the Pacific Coast of the United States.)

latitudes in the Southern Hemisphere than in the Northern Hemisphere.

Where data extend beyond one year, averages for the second year are higher than for the first year. At the South Pole, where the longest record exists, the concentration has increased at the rate of about 1.3 ppm per year. Over the northern Pacific Ocean the increase appears to be approximately 1.0 ppm per year. Since measurements are still in progress, more reliable estimates of annual increase should be available in the future.

At the South Pole, the observed rate of increase is nearly that to be expected from the combustion of fossil fuel (1.4 ppm), if no removal from the atmosphere takes place. This agreement in the observed and expected rates of increase suggests that the oceans have been without effect in reducing the annual increase in concentration resulting from the combustion of fossil fuel. However, since the seasonal variation in concentration observed in the Northern Hemisphere is several times larger than the annual increase, it is also possible that a small change in the factors producing this seasonal variation may also have produced an annual change counteracting any oceanic effect.

Satellite Measurements of Cosmic Dust

The following report is based on material by H. E. LaGow and W. M. Alexander of the National Aeronautics and Space Administration. A more complete version will be published as a NASA Technical Note.

Significant results in the detection of cosmic-dust particles in the vicinity of the earth have been obtained by two US-IGY satellites, 1958 Alpha (Explorer I) and 1959 Eta (Vanguard III). This report deals primarily with the data from 1959 Eta (see *Bulletin No. 28*), comparing them with the earlier findings.

Technique and Instrumentation

Although several environmental sensors were carried on 1959 Eta, preliminary results are ready at this time only for the sensor measuring micrometeoroid impacts. The experimental apparatus consisted of a microphone-impact-counter system utilizing four piezo-electric transducers attached to the metallic skin of the satellite. A collision between the sensitive portion of the satellite surface and a dust particle produced a piezo-electric signal from the microphone system. The electric pulse resulting from an impact was suitably amplified and recorded in a three-digit decimal counter.

Each counter had as its most essential element a "rectangular-loop" type of magnetic core with a hole bored perpendicular to the coil axis. The configuration was named a "cyclops core." Rectangular-loop magnetic cores have the property of retaining any flux level to which they are set. Since the flux level of the cyclops core was changed only by the incoming counts, continuous monitoring of the signal was not necessary to determine the total number of impacts.

The telemetry system used had an output consisting of tone bursts separated by

blank spaces. Information was contained in (a) the length of a tone burst, (b) the frequency of the burst, and (c) the length of time between one burst and the next. The counter information was presented in (b), as follows: the frequency of one tone burst was indicative of the units count, the frequency of a second tone burst indicated the tens count, and a third frequency indicated the hundreds count.

On 1959 Eta, the impactor sensor was calibrated as an impulse-measuring device, which measured a physical parameter of the impacting particle closely related to the particle's momentum. As more knowledge is obtained concerning hypervelocity impact phenomena, the exactness of the calibration of the acoustical devices used in dust particle sensors will be determined and sensitivity threshold levels of reported results can be adjusted, if necessary.

The threshold response of the sensor was determined by dropping very small glass spheres on the sensitive area of 1959 Eta's shell (about 60% of the surface of the spherical portion of the satellite). The mass of these beads was 55 micrograms, $\pm 8\%$, and their velocities were known to an accuracy of $\pm 5\%$. Except for an area of between one and two square inches centered over each microphone, the threshold sensitivity of the total sensitive surface varied between 0.9×10^{-2} and 1.2×10^{-2} dyne-secs. A one-inch-diameter circular disc was mounted over each microphone sensor; thus, for approximately 95% of the sensitive skin, the threshold sensitivity was as determined. The physical dimensions of the surface sensitive to dust-particle collisions was approximately four-tenths of a square meter.

Results

The data that has been reduced represents, primarily, one counter-reading per day.

Because there is an interaction between the magnetometer also carried aboard 1959 Eta and the microphone instrumentation for the micrometeorite experiment, a detailed study of all of the telemetry records must be made before final analysis of the data is complete.

The magnetic-field experiment required a command function from the ground stations, which added a count to the digital counter system on some of the interrogations. All of the satellite interrogations for magnetic-field data occurred when telemetry information was also being received; false counts entered in the counter were monitored and will be subtracted from the real counts. From the data reduced at this time, the average number of false counts per interrogation was determined, and a check was obtained by comparison with three periods

day for the same period as that covered in Figure 10.

In computing the influx rate, an effective area for the impact section of the satellite had to be determined. Tentatively, the impact area is considered to be equivalent to that of a 20-inch-diameter cylinder, 10 inches high, tumbling in space and partially shielded by the earth (shielding effect, approximately 25%). Over the 22-day period depicted in Figure 10, the maximum-minimum variation of any count rate recorded by the impact instrumentation for any 24-hour period is less than a factor of 10.

One of the three periods during the lifetime of the satellite when no interrogations of the magnetometer experiment occurred was September 30, 1959. Sixty-five impacts on the sensitive area of the satellite were

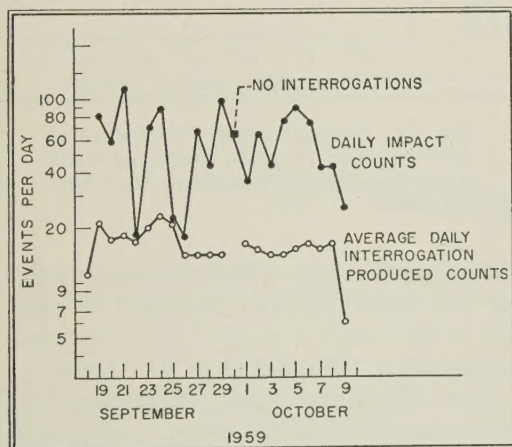


Fig. 10. Preliminary Counts of Daily Impacts and Average Daily Counts Produced by Interrogations for the Period September 18–October 9, 1959.

during the satellite's lifetime when no interrogations were made.

The total daily impact rate and the average daily false pulses due to the interrogations for the period September 18 to October 9, 1959, are shown in Figure 10. Figure 11 shows the corrected impact rate (average daily interrogation pulses subtracted from the total daily count) and the influx rate in impacts per square meter per

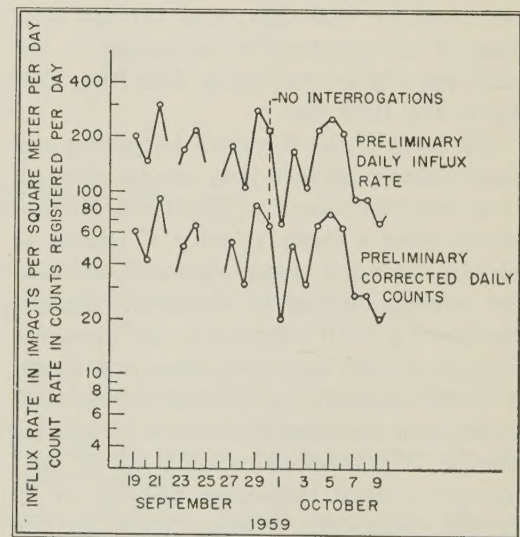


Fig. 11. Preliminary Corrected Daily Impact Counts and Preliminary Daily Influx Rate, September 18–October 9, 1959.

recorded during this 24-hour period. The average count per day for the above 22-day period, after interrogation counts were subtracted, was 45. Thus, the count recorded during the interrogation-quiet period was either higher than normal, or the average number of false pulses being used at this time is too high. It is expected that this

slight ambiguity will be practically eliminated when the complete data records are available.

The influx rate of particles per square meter per day (Fig. 11) ranged from 67 to 300. Figure 4 shows that the daily count rate varied by a factor of approximately 4½. It is felt that the measurement definitely indicates an average influx rate of at least 150 impacts/m²/day. The rate for the interrogation-quiet day was 210 impacts/m²/day.

Discussion

A tentative estimate of the number and mass of interplanetary particles striking the earth per day can be made using the data from 1959 Eta. This is done in terms of (1) the component of interplanetary matter measured by 1959 Eta, and (2) the total mass of micrometeorites impinging on the earth per day by combining data from 1958 Alpha and 1959 Eta.

The mass of the threshold impacting particle (lightest particle that can be counted, at an assumed impact velocity) may be computed using a mean velocity of impact of 30 kilometers per second, the calibration of the system having a threshold impact-impulse of 1×10^{-2} dyne-secs, and assuming that, at meteor velocities, there is a linear, or direct, relationship between the force of impact and the magnitude of the resulting impulse. The threshold mass is 3.3×10^{-9} gms at a mean impacting velocity of 30 km/sec. Using the average figure for the influx rate over the 22-day period and assuming, at the moment, that a significant number of meteoric particles are not in orbit around the earth, the mass influx per day on the earth of this component of interplanetary matter is 6×10^2 tons.

An estimate of the amount of interplanetary matter falling on the earth each day can be obtained from two independent measurements, made by 1958 Alpha and 1959 Eta, which used the same type of sensors and calibration techniques. The

threshold impact-impulse sensitivity of 1958 Alpha was 2.5×10^{-3} dyne-secs. The corresponding threshold mass sensitivity was 8×10^{-10} gms at a mean impact velocity of 30 km/sec. If it is assumed that the measurements by both satellites are valid dust-particle measurements, then, by extending the mass distribution curve defined by these measurements (Fig. 12),

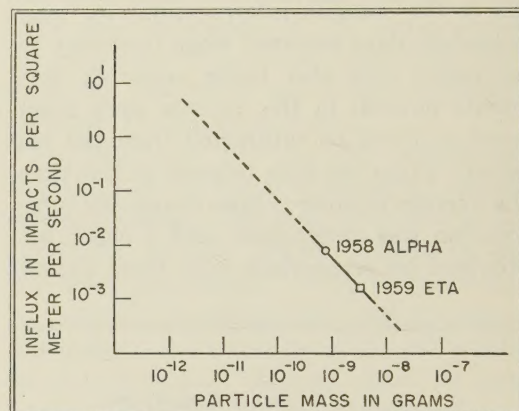


Fig. 12. Tentative Mass Distribution of Micrometeorite Particles, Based on 1958 Alpha Results and Preliminary Data from 1959 Eta.

the daily influx rate of interplanetary matter on the earth between particles of mass 1.2×10^{-8} and 1.2×10^{-10} gms is approximately 10×10^3 tons.

Two additional facts concerning the measurement of interplanetary dust-particle influx by 1959 Eta should be noted. First, the number of actual events counted is the largest yet reported. The total count of impacts for the first 22 days is approximately 1000 (false pulses subtracted), compared with 153 for 1958 Alpha. Second, the area-time product for the lifetime of 1959 Eta was greater than 3×10^{10} cm²-secs, compared with an area-time product of 1.8×10^8 cm²-secs for the earlier satellite.

Satellite 1958 Delta (Sputnik III) had sensors for direct measurement of particle influx. No clear indication of the total number of events or the area-time product has been published to date. However, the

average influx rate has been reported as 1.7×10^{-3} impacts/m²/sec, with a threshold sensitivity of 10^{-9} gms, assuming a mean velocity of the meteor particles of 40 km/sec. Thus, considering the reported influx rates, and the corresponding mass threshold sensitivities of the sensors, the three satellite findings report an influx rate between 1×10^{-3} and 8.4×10^{-3} impacts/m²/sec for mass threshold sensitivities ranging between 3.3×10^{-9} and 8×10^{-10} gms.

A brief comparison of the influx rate obtained by direct measurement techniques on 1959 Eta with the data obtained from various indirect measurement methods can be made. The indirect measurement methods can be classified in two main categories: (1) data obtained by visual and radar observations, and (2) data from considerations of zodiacal light.

Data from the first category contains influx information concerning particles down to a mass of approximately 10^{-5} gms. Various zodiacal-light computations consider particles with diameters from 10 to 300 microns. The data from the various methods in the first category are consistent with each other within a factor of 10. By extrapolating these data to the mass threshold of 1959 Eta, the average influx rate as determined by 1959 Eta is between 100 and 1000 times greater than the data from category one. The different zodiacal-light considerations are consistent with each other within approximately a factor of 100. In comparing these data with those of 1959 Eta, the result varies from an influx rate similar to that of the satellite findings to an influx rate 100 times smaller than that of the satellite measurements.

IGY Bibliographic Notes

The following bibliographic references relating to IGY and IGC-1959 programs and findings were selected from a bibliography under preparation in the Science and Technology Division of the Library of Congress.

- F. Addey: A Note on Roche's Limit. *Journal of the British Astronomical Association*. Vol. 69, no. 6/8, part 2. Oct. 1959. Pp. 292-293, Diagr.
- A. P. Báez: La Medición De La Concentración Del Bióxido De Carbono Del Aire Y El Estudio De Su Difusión, Como Un Medio Para Evaluar La Contaminación Atmosférica. *Ingeniería Química*. Vol. 4, Feb. 1959. Pp. 22-26.
- Diran Deirmendjian and E. H. Vestine: Some Remarks on the Nature and Origin of Noctilucent Cloud Particles. *Planetary and Space Science*. Vol. 1., no. 2. Apr. 1959. Pp. 146-153. Diagr.
- L. Harang and J. Tröim: An Example of Heavy Absorption in the VHF-Band in the Arctic Ionosphere. *Planetary and Space Science*. Vol. 1., no. 2. Apr. 1959. Pp. 102-104. Illus., diagr.
- Robert Howard: Observations of Solar Magnetic Fields. *Astrophysical Journal*. Vol. 130., no. 1. July 1959. Pp. 193-201. Diagr., illus.
- A. S. Jursa, Y. Tanaka and F. LeBlanc: Nitric Oxide and Molecular Oxygen in the Earth's Upper Atmosphere. *Planetary and Space Science* Vol. 1, no. 3. Aug. 1959. Pp. 161-172. Illus., diagr.
- S. A. Korff: Cosmic Ray Neutron Studies. *Nuovo Cimento Supplement*. Vol. 8., no. 2. 1958. Pp. 796-800. Diagr.
- Satoshi Nishizawa, Naoichi Inoue, and Yoshio Akiba: Turbidity Distribution in the Subarctic Water of the North Pacific in the Summer of 1957. *Records of Oceanographic Works in Japan*. Special No. 3. (New Series). Oct. 1959. Pp. 231-241. Diagr.
- B. C. V. Oddie: The Composition of Precipitation at Lerwick, Shetland. *Quarterly Journal of the Royal Meteorological Society*. Vol. 85., no. 364. Apr. 1959. Pp. 163-165. Map.
- J. A. O'Keefe: IGY Results on the Shape of the Earth. *ARS Journal*. Vol. 29, no. 12. Dec. 1959. Pp. 902-904.
- H. K. Paetzold: Observations of the Russian Satellites and the Structure of the Outer Ter-

- restrial Atmosphere. *Planetary and Space Science*. Vol. 1., no. 2. Apr. 1959. Pps. 115-124. Diagr., map.
- N. P. Rusin: Meteorological Processes in the Surface Layer of the Atmosphere in Antarctica U. S. Weather Bureau. Feb. 1960. 31 pp. Diagr., illus. (Translated from *Sovremennye problemy meteorologii prizemnogo sloia vozdukha*, Leningrad, 1958.)
- Paul Siple: *90° South. The Story of the American South Pole Conquest*. New York., G. P. Putnam's Sons. 1959. 384 pp. Illus., diagr., maps.
- J. W. Siry: Satellite Orbits and Atmospheric Densities at Altitudes Up to 750 KM Obtained From The Vanguard Orbit Determination Program. *Planetary and Space Science*. Vol. 1., no. 3. Aug. 1959. Pp. 184-192. Diagr.
- G. E. Taylor: Satellite Altitude, Ground Distance, and Height Graphs. *Journal of the British Astronomical Association*. Vol. 69., no. 5. Aug. 1959. Pp. 217-218. Diagr.
- The Ordinary General Meeting of the Association Held on Wednesday, 1959 February 25, at Burlington House, London, W#1. *Journal of the British Astronomical Association*. Vol. 69., no. 5. Aug. 1959. Pp. 186-189, 194-195.
- U. S. Joint Publications Research Service. Poland's Participation In The International Geophysical Year. *JPRS/NY*. Rept. no. 353. Apr. 14, 1958. 14 pp.
- Harry Wexler: Seasonal and Other Temperature Changes in the Antarctic Atmosphere. *Quarterly Journal of the Royal Meteorological Society*. Vol. 85., no. 365. July 1959. Pp. 196-208. Diagr., map.

SUBSCRIPTION NOTICE

Publication of the *IGY Bulletin* is being continued. Reduction and analysis of the great volume of data accumulated in the course of IGY and IGC-59 programs in geophysics and space research is still proceeding, producing many significant reports on new findings. Moreover, successor world-wide geophysical and space programs are adding to the store of data and new knowledge. The *Bulletin* will continue to report results of these programs.

Present subscriptions terminate with *Bulletin No. 36*, June 1960. Accordingly, *present subscribers must renew their subscriptions* in order to receive issues of the *Bulletin* published after June 1960. The renewal period extends from July 1960 (No. 37) through June 1961 (No. 48). In addition, new subscriptions are available for those wishing all issues of the *Bulletin* from July 1957 through June 1961. Rates are as follows:

	Renewals and new 1-year subscrip- tions (12 issues)	New complete- set subscrip- tions (48 issues)
Science teachers and students		
a) Single subscriptions	\$1.50	\$6.00
b) 5 or more mailed to a single address	1.00	4.00
Other subscriptions	2.00	8.00

Please send remittances to the Printing and Publishing Office, National Academy of Sciences, 2101 Constitution Avenue, N.W., Washington 25, D. C. Make checks payable to the National Academy of Sciences. Include purchase orders if necessary.